UDC 551.576.1:551.558.1:551.515.51(213)

Cumulus Convection and Larger Scale Circulations
II. Cumulus and Mesoscale Interactions

RAUL ERLANDO LOPEZ [1]—*Department of Atmospheric Science, Colorado State University, Fort Collins, Colo.*

ABSTRACT—This paper (part II) is the second of two papers dealing with cumulus and broader scale flow interaction. The first (part I) is a companion paper that deals with this topic from broad-scale considerations. The second (part II) deals with this topic from the cumulus scale point of view.

A numerical model of individual convective clouds has been used to investigate the effects of a typical population of cumulus clouds on the large-scale features of a tropical disturbance or cloud cluster. The typical cloud population has been determined from U.S. Navy aircraft reconnaissance radar data in the tropical Atlantic Ocean.

This study shows that the detrainment of cloud mass from the population produces net cooling of the air around the clouds. This occurs because the cooling produced by the evaporation of the detrained cloud liquid water overcompensates for the detrainment of sensible heat excess. A heat and moisture budget for a steady-state tropical cloud cluster has been computed using the typical cloud population. A mass budget of the cluster reveals that the vertical circulation required to explain typically observed rainfall rates has a magnitude many times larger than the synoptic mass circulation. The synoptic scale vertical mass circulation is, in fact, a small residual between both the much larger upward mass transport by the clouds and the downward mass transport induced in the cloud-free region around the clouds.

1. INTRODUCTION

Parameterization of the effects of cumulus convection on larger scale circulations is perhaps one of the most important current problems in meteorology. To attack this problem, we should first investigate three aspects of cumulus convection:

1. The behavior of individual clouds.
2. The size distribution of clouds present in different convective systems.
3. The role of cumulus clouds in the heat and moisture budget of different cloud systems.

Corresponding to the first aspect, a new numerical model of individual cumulus clouds has been developed by the author (López 1973—designated as paper A).[2] The model has been designed with the specific purpose of simulating those aspects of cumulus convection that are important to the cloud-environment interaction processes. In the present paper, the second aspect of cumulus convection will be explored by applying the results of the numerical cloud model in paper A to radar data representative of tropical cloud clusters. The resulting typical cloud population in turn is used to investigate the third aspect by performing a heat and moisture budget of a mean tropical disturbance or cloud cluster.[3] The main objective here is to ascertain the mechanisms by which cumulus clouds impart heat to their environment for the maintenance of the energy budget of tropical disturbances.

The statement that cumulus convection produces the energy necessary for hurricane development is generally accepted; however, the mechanism by which cumulus clouds impart their energy to their environment is imperfectly understood. Also generally accepted is the concept that the frictionally induced vertical velocity at the top of the boundary layer produces a flux of low-level air that rises in cumulus towers. As condensation takes place, the temperature of these ascending currents will be higher than the environment. This excess enthalpy is then assumed to be imparted to the surrounding clear air by the detrainment process.

The excess sensible heat that a cloud parcel has at a given time, however, is not available to the environment in its entirety. Most of it is converted into potential energy as the warmer parcel continues to rise. Only a fraction of this heat is given directly to the environment when part of the cloud mass is detrained to the exterior. This exportation of sensible heat from the cloud, however, is counteracted by the simultaneous cooling produced by the evaporation of the detrained cloud water. The net result of the detrainment of cloud mass may even result in the cooling of the cloud's environment.

Another way in which cumulus clouds interact with their environment is by generating local mass sources and sinks by virtue of their large upward mass transport. As a result, a cloud produced convergence-divergence field is imposed on the environment. A compensatory downward transport of mass will be induced in the cloud-free regions. With the usually stable stratification of the

[1] Now at the Institute of Tropical Meteorology, Department of Physics, The University of Puerto Rico, Rio Piedras, Puerto Rico

[2] This model was first presented in the form of a project report (López 1972).

[3] The terms "tropical disturbance" and "cloud cluster" are used interchangeably in this paper. For a more precise definition, refer to figure 3 in part I by Gray (1973).

Tropics, considerable compressional warming can result from the descending branch of the convective circulation.

The investigations presented in this paper are directed toward a better understanding of the magnitude and relative importance of each of these two cumulus-induced processes in the maintenance of the energetics of tropical disturbances.

2. CLOUD MODEL

The model used in these investigations is Lagrangian, time dependent, one dimensional, and parametric. (For a detailed description, see López 1973.) *The Lagrangian scheme* works as follows: A cloud in the model is started by generating a series of boundary-layer parcels that go up one after the other through cloud base during a given forcing period. Each of these parcels is followed in time in a Lagrangian way. Thus at a given moment, a cloud consists of a vertical stack of parcels that were generated at cloud base at different times. The equations of motion, thermodynamics, water substance, and mass continuity are solved for each of the parcels at every time step. These different cloud parcels are not isolated; instead, they are allowed to interact with one another by means of a vertical exchange of mass and rain particles. This treatment is capable of simulating vertical profiles of temperature, moisture, liquid water content, and vertical velocity for the entire depth of the cloud.

The model is *Time dependent;* thus the entire depth of the cloud is simulated throughout its complete life cycle of growth, maturity, and decay. Each of the cloud parcels is followed in time until it is incorporated into the environment, at the time when it has no liquid water present and its vertical velocity is of the same order of magnitude as the environment's turbulence intensity.

Although the formulation of the model is basically *one dimensional,* the clouds are assumed to consist of two interacting axisymmetrical regions—a protected core and an exposed surrounding shell. Mixing with the environment thus proceeds in two steps—environment to shell and shell to core. In addition to this turbulent mixing between shell and core, mass is exchanged between the two by means of subcloud-scale circulations inside the cumuli. This is modeled in the following way. The shell and the cap of the cloud slow down because of their more direct mixing with the environment. This generates vertical velocity shears across the cloud. We assumed that shears result in an internal circulation of the cloud that is parameterized in terms of a Hill's vortex model. Because of this vortex circulation, mass from the core moves out and down, feeding mass into the shell. Eventually, the cloud turns itself inside out (the old core being exposed) while the cloud mass that was the shell before becomes the new core, and so on. The radii of the core and shell parcels are part of the predicted variables, which (of course) vary with both time and height; thus the cloud's profile is known at every time step.

The mixing between cloud and environment is *parameterized* in the model in terms of the turbulence intensity of the interior and exterior of the cloud. In this way, the entrainment and detrainment rates are not proportional to the cloud scale (or mean) vertical velocity of the cloud; instead, they are proportional to the root-mean-square (rms) of the velocity fluctuations inside and outside the cloud. By doing this, we avoid the commonly used but physically invalid assumption of similarity. Additional equations have been introduced in the model to predict the turbulence level of the different cloud parcels at all times.

In general, all these improvements allow a more realistic representation of the dynamics of cumulus clouds and of the total rainfall produced by the individual convective elements than has been heretofore possible with other one-dimensional parametric models. The present model has been developed to serve as a tool in the investigation of the interaction of cumulus convection with the large-scale circulations. For this reason, the model has been designed to be much simpler and less time consuming than existing two-dimensional hydrodynamic models of cumulus clouds.

3. EFFECTS OF CLOUDS ON ENVIRONMENT

Cloud Detrainment

As a cloud grows and decays, some of its mass is given off to the environment by the process of detrainment. In this way, excess sensible heat, liquid water, and water vapor are exported to the surrounding air. The magnitude of these transports depends on the rate of mass detrainment and on the thermodynamic properties of the cloud; thus the rate at which a layer of an individual cloud gives off *excess* sensible heat can be expressed as

$$\frac{d\mathcal{Q}}{dt}=c_p(T'-T'')\frac{dm_d}{dt}. \tag{1}$$

Here, the prime refers to the cloud, the double prime to the environment; dm_d/dt is the detrainment rate for the cloud layer; and $\mathcal{Q}$ represents sensible heat. Similarly, the rates at which cloud air, *excess* water vapor, and liquid water are given to the environment by a cloud segment can be written as

$$\frac{dm_a}{dt}=\frac{dm_d}{dt}, \tag{2}$$

$$\frac{dm_v}{dt}=(x_v'-x_v'')\frac{dm_d}{dt}, \tag{3}$$

and

$$\frac{dm_w}{dt}=\frac{Q_{cl}}{\rho}\frac{dm_d}{dt}. \tag{4}$$

In these expressions, x refers to the mixing ratio of water vapor; Q_{cl}, the cloud liquid water content; and m_v and m_w, the mass of water vapor and liquid water, respectively.

Now consider a group of active cumulus clouds. Assume this field of clouds is surrounded by a large vertical cylinder of radius R, which extends from the surface to the

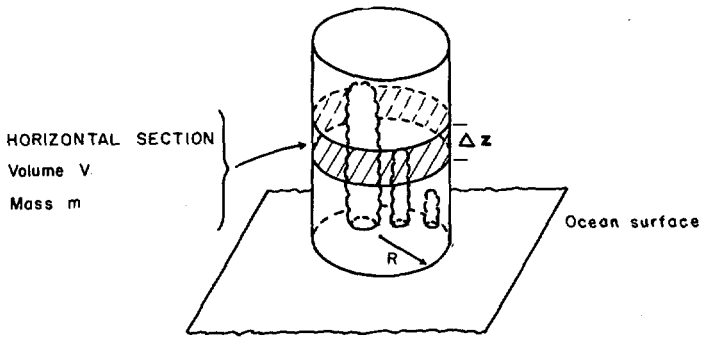

FIGURE 1.—Geometrical model for the computations of the effect of cumulus clouds on the surrounding environment.

level of the tropopause. This cylinder is divided into horizontal layers of height, Δz, and mass, m (fig. 1). The rate at which a layer of this enclosing cylinder receives excess sensible heat from the clouds can be obtained by adding the excess heating rates produced by each of the cloud segments contained in the layer. Thus (1) becomes

$$\frac{d\mathcal{Q}}{dt}=\sum_{\substack{\text{all}\\ \text{cloud}\\ \text{segments}\\ \text{in the}\\ \text{layer}}} c_p(T'-T'')\frac{dm_d}{dt}. \tag{5}$$

The total excess heating of the cylinder layer during a long period of time, Δt, can be obtained by integrating eq (5) with respect to time. Thus

$$\Delta\mathcal{Q}=N_1\int_0^{\tau_1} c_p(T'-T'')\frac{dm_d}{dt}\,dt + N_2\int_0^{\tau_2} c_p(T'-T'')\frac{dm_d}{dt}\,dt+\cdots \tag{6}$$

where N_i is the total number of clouds of type i that existed during the time interval, Δt, and τ_i is the lifetime of cloud type i. We have assumed that $\Delta t>>\tau_i$. N_i is dependent on the total low-level mass available to form clouds of type i and on the amount of subcloud-layer mass that a cloud of type i uses during its growth period. The mass channeled into clouds of type i from the subcloud layer during the time interval Δt is given by

$$\Delta m_i=-\alpha_i\nabla\cdot\mathbf{V}_0\rho_0 B\pi R^2\Delta t \tag{7}$$

where $\nabla\cdot\mathbf{V}_0$ is the subcloud-layer convergence into the clouds of the disturbance; ρ_0, the density of the subcloud layer; B, the height of cloud base; R, the radius of the cylinder enclosing the disturbance; and α_i, the fraction of the total mass convergence going into clouds of type i. The subcloud-layer mass used up by a cloud of type i during its growing stage is given by

$$\delta m_i=\int_0^{t_0}\rho_0\pi r_0^2 w_0\,dt \tag{8}$$

where r_0, w_0, and t_0 are the radius, velocity, and duration of the updraft through cloud base, feeding the clouds during its growing stage. Thus N_i, the number of clouds of type i, can now be obtained as

$$N_i=\frac{\text{Total mass available from subcloud layer}}{\text{mass used by cloud } i \text{ during its growing stage}}$$

or

$$N_i=\frac{\Delta m_i}{\delta m_i}=-\alpha_i\frac{\nabla\cdot\mathbf{V}_0\rho_0 B\pi R^2\Delta t}{\int_0^{t_0}\rho_0\pi r_0^2 w_0\,dt}. \tag{9}$$

Equations similar to (6) can be readily derived for the increase in air mass, excess water vapor, and liquid water produced by the process of detrainment for a layer of the cylinder surrounding the clouds. These equations have the form:

$$\Delta m_a=N_1\int_0^{\tau_1}\frac{dm_d}{dt}\,dt+N_2\int_0^{\tau_2}\frac{dm_d}{dt}+\cdots, \tag{10}$$

$$\Delta m_v=N_1\int_0^{\tau_1}(x'-x'')\frac{dm_d}{dt}\,dt+N_2\int_0^{\tau_2}(x'-x'')\frac{dm_d}{dt}\,dt+\cdots, \tag{11}$$

and

$$\Delta m_w=N_1\int_0^{\tau_1}\frac{Q_{cl}}{\rho}\frac{dm_d}{dt}\,dt+N_2\int_0^{\tau_2}\frac{Q_{cl}}{\rho}\frac{dm_d}{dt}\,dt+\cdots. \tag{12}$$

The net change in temperature due to detrainment alone for a section of the enclosing cylinder is produced by the combined effect of the direct detrainment of sensible heat and the evaporation of the liquid water detrained from the clouds at the same time. Thus the rate of temperature change of the layer by detrainment alone can be expressed as

$$\frac{\Delta T}{\Delta t}=\frac{1}{(m+\Delta m_a)c_p}\frac{\Delta\mathcal{Q}}{\Delta t}-\frac{L}{(m+\Delta m_a)c_p}\frac{\Delta m_w}{\Delta t} \tag{13}$$

where L is latent heat. Similarly, the rate of moisture alteration due to detrainment is

$$\frac{\Delta x}{\Delta t}=\frac{1}{(m+\Delta m_a)}\frac{\Delta m_v}{\Delta t}+\frac{1}{(m+\Delta m_a)}\frac{\Delta m_w}{\Delta t}. \tag{14}$$

In these formulas, m is the mass of the layer of the enclosing cylinder and is defined as

$$m=\rho\pi R^2\Delta z. \tag{15}$$

Evaluation of Net Heating and Moisture Alterations

Before eq (13) and (14) can be evaluated using the cloud model of paper A, the subcloud-layer convergence into the clouds, $\nabla\cdot\mathbf{V}_0$, and the distribution of cloud types, α_i, must be specified as external conditions. Although the radius of the enclosing cylinder and the averaging time interval Δt enter into the numerator of eq (9), these quantities do not have to be specified in

the final evaluation of the heating and moisture-alteration rates [see eq (13)–(15)].

The frequency distribution of the different cloud types, α_i, will be obtained from radar data representative of tropical cloud clusters presented in the next section. If all the cumulus within the cluster had to be sustained by the synoptic convergence of only $3\text{–}5\times10^{-6}$ s^{-1}, then low-level mass requirements would permit only ~1/500 to 1/1000 of the cluster area to be occupied by such clouds (López 1968, Williams and Gray 1973). The actual convergence of mass into the clouds of a disturbance (or cloud cluster), however, is probably several times larger than these values. The downdrafts generated by cloud growth and evaporation of rain will obscure the true value of the low-level mass convergence available for cloud formation (Riehl and Malkus 1958, Gray 1973). If the rain-producing efficiency of the cloud population of a disturbance is known, an estimate of the actual low-level convergence into the clouds ($\nabla \cdot \mathbf{V}_0$) could be obtained from the associated rainfall data. In the case of the cumulonimbus simulated in paper A, for example, the total rain produced was 240 acre-ft (3.0×10^{11} g of water) while the total mass of subcloud-layer air flowing into the cloud throughout its growing stage was $\delta m=5.6\times10^{13}$ g [eq (8)]. On the other hand, Williams and Gray (1973) calculated a mean rainfall of 2.5 cm/day for tropical cloud clusters over a 4° latitude square area. This corresponds to a total mass of water of $2.5A$ g/day where A is the area of the disturbance or cloud cluster. This means that a total of $N=2.5\ A/3.0\times10^{11}$ cumulonimbi of the type simulated in paper A would be needed to provide the observed daily rainfall if only that type of cloud is assumed to be present in the disturbance. The total mass of subcloud-layer air needed for the growth of those clouds in 1 day would be then $N\delta m$. This amount of low-level mass must be supplied to these particular clouds in 1 day to account for the typically observed rainfall rates. Thus from eq (7),

$$\Delta m=-\nabla\cdot\mathbf{V}_0\rho_0BA\Delta t=N\delta m$$

where Δt is an interval of 1 day. The equivalent low-level convergence into the clouds of the cluster can now be evaluated as

$$-\nabla\cdot\mathbf{V}_0=0.94\times10^{-4}\text{s}^{-1}.$$

The towering and small cumulus simulated in paper A would similarly require convergences of 5.8×10^{-4}s^{-1} and 1.6×10^{-3}s^{-1} if the cloud population of the disturbance was composed of only clouds of their type.

These convergences are much larger than the synoptically evaluated ones. The actual magnitude of the convergence of mass into the growing clouds, however, hinges on the rain-producing efficiency of the convective system (i.e., how much subcloud moisture is needed to produce 1 g of rain water) and the mean rainfall rate over the area of the disturbance. The more efficient precipitator a cloud is, the less convergence of water vapor is needed to produce the same amount of rain. In the case of our simulated cumulonimbus, the efficiency is 40 percent, which would put this cloud in the category of "efficient", and thus put the computed convergence values on the conservative side. Similarly, a rainfall rate of 2.5 cm/day for a tropical disturbance is not large. Thus a mass convergence into the sub-cloud layer of 10^{-4}s^{-1} does not seem unrealistic. For illustration, this last figure will be used in the computation of the heating and moisture-alteration rates for the typical cloud population.

If the observationally evaluated synoptic convergences of 10^{-6} to 10^{-5}s^{-1} are real, most of the large mass required for the growth of clouds, as computed above, must come from subsynoptic sources (viz, the compensatory subsidence induced around the individual growing clouds). This extra vertical exchange may be very significant in the momentum and heat budget of tropical cloud clusters.

Convergence-Divergence Pattern Induced by Clouds

The vertical transport of mass by individual clouds produces local mass sources and sinks that are reflected on the environment as regions of horizontal divergence and convergence. At any particular level, the magnitude of this horizontal divergence field will depend on the change of mass of the individual clouds present at that location. In turn, the rate at which the mass of a layer of an individual cloud changes is determined by the internal vertical advection of mass and by the mass gained and lost through entrainment and detrainment. Thus

$$\frac{dm}{dt}=\left(\frac{dm}{dt}\right)_{\text{Advection}}+\left(\frac{dm}{dt}\right)_{\text{Entrainment}}-\left(\frac{dm}{dt}\right)_{\text{Detrainment}} \quad (16)$$

Now consider a group of clouds surrounded by the same control volume used before. The combined change in mass experienced by all the cloud segments contained in a layer of the enclosing cylinder can be expressed as

$$\frac{dm}{dt}=\sum_{\substack{\text{all cloud}\\ \text{segments}\\ \text{in the layer}}}\frac{\delta m}{\delta t}. \quad (17)$$

By integrating eq (17) over a long period of time, Δt, the total mass change experienced by the clouds can be expressed as

$$\Delta m=N_1\int_0^{\tau_1}\frac{dm}{dt}\,dt+N_2\int_0^{\tau_2}\frac{dm}{dt}\,dt+N_3\int_0^{\tau_3}\frac{dm}{dt}\,dt+\ \ldots \quad (18)$$

where the different symbols have the same meaning as before.

The divergence due to the cloud's vertical mass transport in the layer of the cylinder during a large period

of time, Δt, can now be expressed as

$$\nabla \cdot \mathbf{V} = -\frac{1}{m}\frac{\Delta m}{\Delta t} \tag{19}$$

where m is given by eq (15). If the values of Δm, m, and N_i from eq (18), (15), and (9) are introduced in eq (19), the expression for the horizontal divergence of the layer due to the clouds becomes

$$\nabla \cdot \mathbf{V} = -\frac{\nabla \cdot \mathbf{V}_0 B}{\rho \Delta z \int_0^{t_0} \pi r_0^2 w_0 dt} \times \left[\alpha_1 \int_0^{\tau_1} \frac{dm}{dt} dt + \alpha_2 \int_0^{\tau_2} \frac{dm}{dt} dt + \alpha_3 \int_0^{\tau_3} \frac{dm}{dt} dt + \ldots\right]. \tag{20}$$

Equation (20) will be evaluated by using the cloud model of paper A to compute the geometry and the entrainment and detrainment rates of different cloud types. The cloud distribution and the value of the subcloud-layer mass convergence will be the same as those that will be used to evaluate the corresponding heating and moisture alteration rates [eq (13) and (14)].

4. MODEL CLOUD POPULATION

Radar Information

A realistic assessment of the role of convection in the heat and moisture budgets of tropical storms should take into consideration the type of cumulus population present in the disturbance. The combined effect of all the convective elements depends on the proportion in which the different cloud types are present. For example, if most of the low-level moisture convergence is channeled into small cumuli, only a fraction of the storm's latent heat input can be realized as sensible heat. Not only is the magnitude of the latent heat release dependent on the cloud population but also its distribution with height. Although cumulus convection is of utmost importance to the energetics of disturbances, very little effort has been devoted to investigating the types of clouds present in tropical cloud clusters. Holle (1968) has performed some studies on tropical oceanic cloud populations. He, however, did not intend to answer the question of what are the different types and relative frequencies of cumulus clouds present in a disturbance at a given time.

During the 1968 Barbados Meteorological Experiment, the author flew with the Navy's Weather Reconnaissance Squadron Four into about a dozen tropical cloud clusters in the West Indies region. The scope of the 10 cm (APS 20) airborne radar was photographed on every other scan. From these automatic picture sequences, the lifetimes of the new individual echoes that appear on the scope every 5 min have been estimated. Groups of individual echoes have not been considered. Very large echoes are probably composed of several individual cells, and their lifetimes would not be representative of individual convective elements. We felt that, by considering only individual isolated echoes, we could obtain a frequency distribution of echo duration representative of the entire population of convective elements, whether they appear singly or in clusters. The histogram of Figure 2 was constructed from more than 600 such individual echoes. This echo lifetime distribution is typical of all the disturbances encountered. Several different stratifications of the data were tried (e.g., cloud cover amount, surface pressure, latitude, range, and time of day) with no significant departure from the form of the overall average distribution.

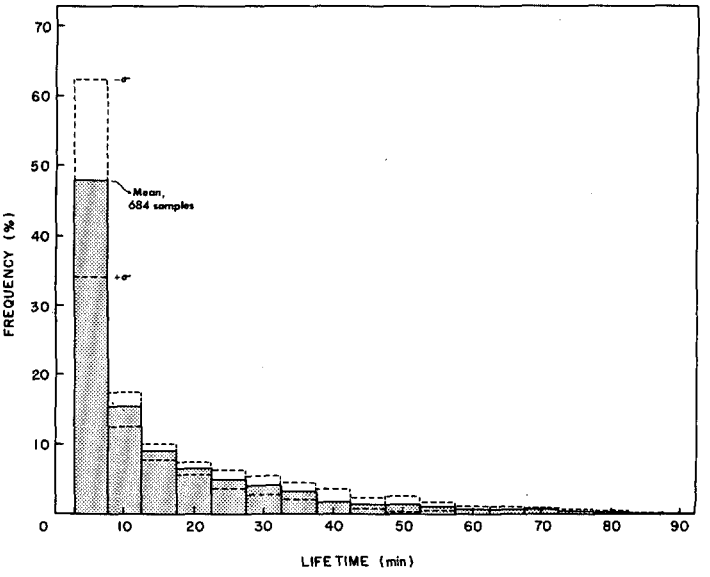

FIGURE 2.—Frequency distribution of echo lifetimes.

The average echo lifetime for all the data is 14.5 min. This value is smaller than the average of 32 min for hurricanes obtained by Senn et al. (1959) and 35 min obtained by Senn and Stevens (1965). They, however, did not consider echoes of short duration ($\leq$10 min). On the other hand, McIntyre (1956) has found 17 min to be the average for hurricane cumuli by tracing echoes that lasted from 4.5 to 46 min. Nevertheless, these previous studies and the present one agree that both hurricanes and tropical cloud clusters contain many more short-lived echoes than long-lived ones. A similar conclusion can also be derived from echo lifetime distributions obtained for middle latitudes for both winter and summer storms (Blackmer 1956, Battan 1953).

One reasonably can assume that the long-lived echoes are generally wider and taller than the short-lived ones (Battan 1953, Senn and Stevens 1965). The present data do not allow us to measure accurately the horizontal and vertical sizes corresponding to the different lifetime categories. The available evidence, however, suggests that the longer lived echoes are indeed generally wider and taller than the short-lived ones. This evidence would tend to indicate that the cloud populations of tropical disturbances are composed of a majority of small cumuli, some towering cumuli, and a few cumulonimbus towers. Thus a large portion of the latent heat contained in the low-level moisture input is not realized as sensible heat because condensation in clouds of small vertical extent is severely limited. This fact must be taken into consideration

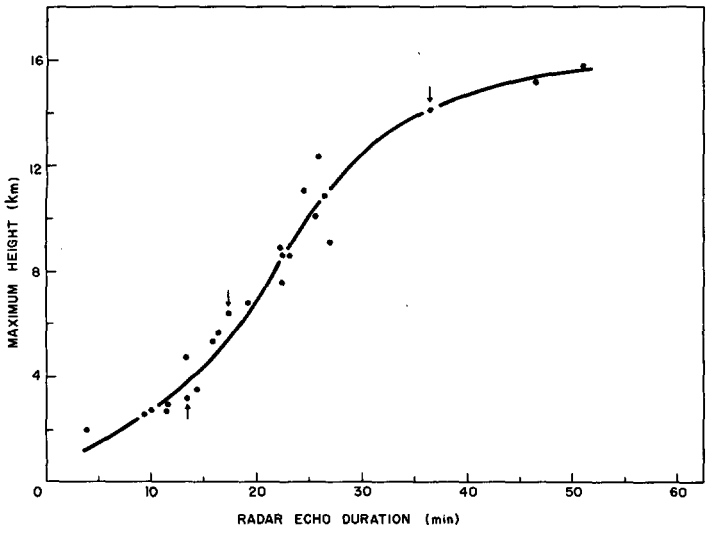

FIGURE 3.—Relationship between radar echo duration and the maximum height attained by clouds simulated with the numerical model of paper A (López 1973) by assuming different initial conditions. The arrows identify the three typical clouds described in paper A.

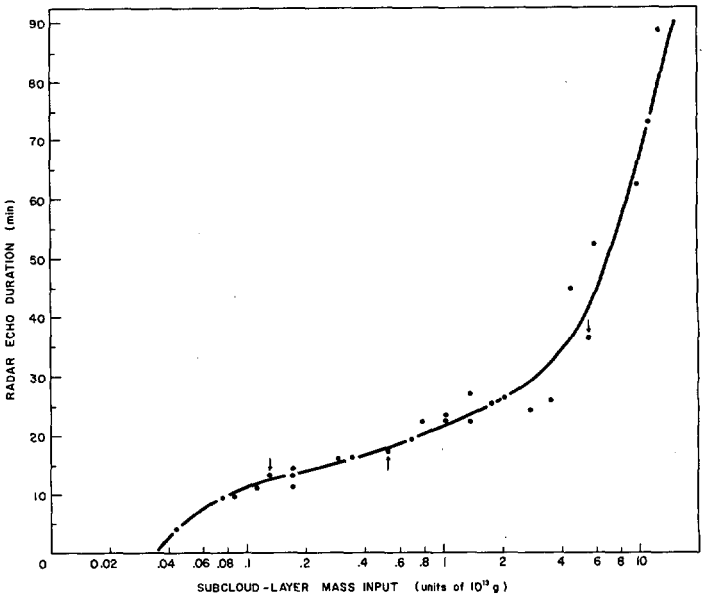

FIGURE 4.—Relationship between radar echo duration and the total subcloud-layer mass input for clouds simulated with the numerical model of paper A by assuming different initial configurations. The arrows identify the typical clouds described in paper A.

if the effect of cumulus convection on tropical cloud cluster energetics is to be properly evaluated.

Cloud Population From Radar and Numerical Model Data

Although few in number, there are some clouds in figure 2 that produce echoes of very long duration (50–90 min). One or two of such long-lived echoes were detected in each of the disturbances considered in this study. To produce these persistent echoes, one probably needs a local source of low-level mass of long duration. With the numerical cloud model, we have been able to produce radar echoes lasting 40 to 50 min by maintaining an 8-km-wide updraft through cloud base for 40 min, with a peak speed of 5 m/s. To visualize such a persistent low-level mass flux is difficult unless one postulates the existence of a strong mesoscale organization of the subcloud layer. When considering echoes of long duration, we are probably dealing with cloud systems that have organized the planetary boundary layer so that it can provide a constant source of low-level mass for the close reformation of individual convective cells of a shorter lifespan. The simulation of such a mesoscale cloud system is beyond the scope of the cloud model used in this study. Thus we will assume that the effect on the environment of a cloud having a 60-min radar echo is equivalent to the effect produced by two clouds having a 30-min echo; similarly, a 90-min echo cloud will be represented by three 30-min echo clouds, and so on.

Using the results of the cloud model developed in paper A, we can obtain some information about the distribution of cloud sizes corresponding to the echo lifetime distribution of figure 2. Thus figure 3 has been prepared from the results of the numerical model by plotting the radar echo duration versus the maximum height attained by clouds of different initial conditions. For this diagram, we assumed that the minimum reflectivity, Z, detected by the radar corresponds to 30 dB (10 Log_{10} Z). The close correlation between maximum cloud height and echo duration (fig. 3) indicates that clouds exhibiting long-lived echoes penetrate high into the troposphere. The maximum height obtained by a cloud, however, is not a good representation of its overall size—clouds with small initial radii can rise to high altitudes providing that the initial forcing is intense and of long duration. On the other hand, the total mass of subcloud-layer air flowing into a cloud during its growing stage is a better indication of the overall size of a convective element. Figure 4 shows the duration of the radar echo as a function of the total subcloud-layer mass input for clouds of different initial configuration; for facility of presentation, the abscissa has been plotted on a logarithmic scale. Values of 0.4–2.2 km have been used for the initial radius, 5–20 min for the growth period, and 2.5–5.5 m/s for the maximum updraft velocity through cloud base. Clouds having radar echoes lasting more than 40 min have been composed of two or three clouds with shorter lived echoes. A good correlation exists between echo duration and the amount of mass necessary for cloud growth. Note that there is a rapid decrease in echo duration with decreasing mass input for the smaller clouds (those utilizing 0.1×10^{13} g do not produce detectable radar echoes). In comparison, clouds having very long radar echoes require large amounts of subcloud-layer mass to grow.

Using the curve of figure 4 and the radar information in figure 2, we developed a typical cloud population for trade wind tropical disturbances. This population is shown in figure 5 as the frequency distribution of classes of clouds having different amounts of subcloud-layer mass inputs during their growth stages. The class intervals of the distribution of echo duration (fig. 2) have

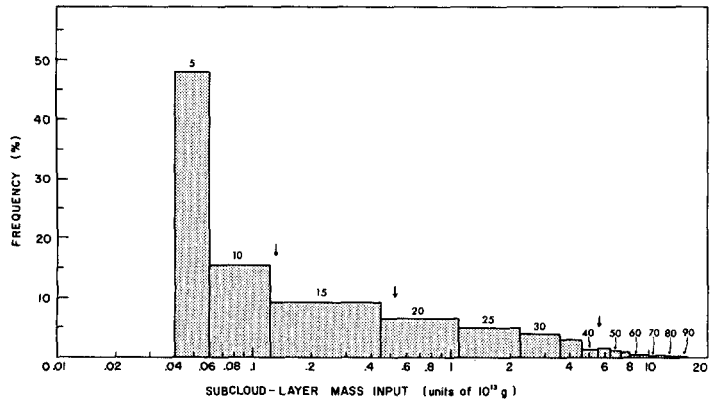

FIGURE 5.—Typical cloud population for the trade-wind tropical cloud cluster shown as a frequency distribution of classes of clouds using different amounts of subcloud-layer mass during their growth stages. The mass-input classes correspond to the echo lifetime classes of figure 2. The arrows identify the three typical clouds described in paper A.

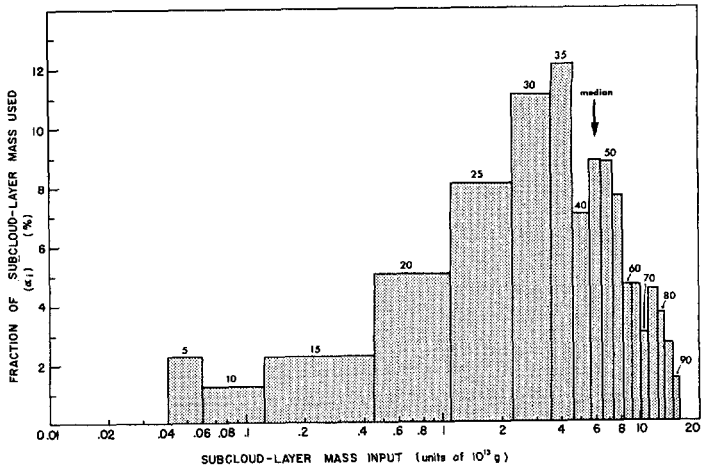

FIGURE 6.—Mass used by different classes of clouds as a fraction of the total subcloud-layer mass available for cloud formation. The cloud classes are expressed in terms of the subcloud-layer mass used in their growth stages. The classes correspond to the echo lifetime classes of figure 2. The large arrow indicates the median of the distribution.

been translated in terms of subcloud layer mass-input classes using the relationship between lifetime and mass-input given by figure 4. From this diagram, one can see that the majority of the clouds in a tropical disturbance are small, processing individually only a very small amount of subcloud-layer air. The few large clouds, on the other hand, process a large amount of subcloud-layer mass during their growth stages. The relative importance of the collective effect of the clouds in each category can be obtained by computing from figure 5 the mass used by each class as a fraction of the total subcloud-layer mass utilized by all clouds in the population. The results of this computation are portrayed in figure 6. The large arrow indicates the median of the frequency distribution i.e., 50 percent of the clouds in the population use more and 50 percent of the clouds in the population use less subcloud-layer mass than the median cloud type. Note also that the largest 50 percent of all the clouds process approximately the same amount of low-level mass as the smallest 50 percent. Although less important individually, the small clouds (because of their large numbers) have as much participation in the vertical mass and energy transports out of the boundary layer as the larger but less frequent cloud cells.

The α_i of eq (11), (12), and (20) are the ordinate of figure 6 (i.e., the fraction of the total low-level mass convergence going into the different classes of clouds). Using these values of α_i, we can evaluate the combined effect of the typical cloud population from these equations. A representative cloud from each of the classes of figure 6 has been used. The characteristics and defining parameters of each of these clouds are listed in table 1. For each type of cloud, the corresponding radar echo lifetime class is listed together with the actual echo duration; radius, duration, and peak speed of the generating impulse; maximum height attained; accumulated rain; percent of total subcloud-layer mass used by the cloud class; and subcloud-layer mass used by the typical cloud. Notice that clouds having echoes lasting 45 min or more have been assumed to consist of two or three cells of shorter echo duration.

We emphasize at this point that the purpose in developing this typical cloud population is to obtain an *order of magnitude estimate* of the effects of an ensemble of different types of cumuli on the atmosphere of a disturbance. The limitations imposed by the quality of the radar data, the accuracy of the numerical model, and the assumptions about the structure of large embedded cloud systems do not warrant the use of this derived cumulus population for detailed energy balances of tropical storms. With these restrictions in mind, the typical cloud population will now be used to compute the alteration rate of temperature, moisture, and mass produced on the synoptic scale of a tropical cloud cluster as the result of sustained cumulus convection.

5. INTERACTION OF A MODEL CLOUD POPULATION WITH SYNOPTIC FEATURES OF A TYPICAL TROPICAL DISTURBANCE

The model cloud population described in section 4 will now be used to investigate the interaction of an ensemble of cumulus clouds with the synoptic flow features of a tropical cloud cluster. The interaction between cloud and synoptic scales takes place in two reciprocal directions. First, the large-scale synoptic flow and the static stability of a disturbance determine the different types of cumulus clouds that will be produced and the numbers in which they will be present. Second, once the cloud population is established, the large-scale fields of temperature, moisture, and momentum will be altered and controlled by the collective influence of the individual clouds.

The first type of interaction has been tacitly incorporated in the characterization of the model cloud population: Here, the types of clouds present and their relative frequencies were obtained from radar observations;

TABLE 1.—*Characteristics of the typical clouds of a tropical disturbance*

Class number	Radar echo duration class	Actual radar echo duration	r_0	T_0	w_0	Max. height	Accum. rain	α_i	δm_i
(*i*)	(min)	(min)	(m)	(min)	(m/s)	(m)	(acre-ft)	(%)	(10^{12}g)
1	5	4.0	500	5	2.5	2,032	0.05	2.30	0.044
2	10	9.5	466	10	2.5	2,645	.13	1.28	.076
3	15	16.0	924	10	2.5	5,352	1.44	2.30	.297
4	20	20.0	1,000	20	2.5	6,759	5.35	5.05	.696
5	25	25.5	1,833	15	2.5	10,111	30.66	8.16	1.754
6	30	26.0	2,247	20	2.5	12,347	80.72	11.08	3.514
7	35	26.5	2,000	20	5.5	14,115	240.14	12.17	5,568
8	40	36.5	2,000	20	5.5	14,115	240.14	7.06	5.568
9(6+4)	45	46.0	2,247	20	2.5	12,347	86.07	8.91	4.210
			1,000	20	2.5	6,759			
10(7+3)	50	52.5	2,000	20	5.5	14,115	241.58	8.88	5.865
			924	10	2.5	5,352			
11(7+3)	55	52.5	2,000	20	5.5	14,115	241.58	7.67	5.865
			924	10	2.5	5,352			
12(7+6)	60	62.5	2,000	20	5.5	14,115	320.86	4.70	9.082
			2,247	20	2.5	12,347			
13(7+6)	65	62.5	2,000	20	5.5	14,115	320.86	4.70	9.082
			2,247	20	2.5	12,347			
14(7+7)	70	73.0	2,000	20	5.5	14,115	480.28	3.11	11.136
			2,000	20	5.5	14,115			
15(7+7)	75	73.0	2,000	20	5.5	14,115	480.28	4.59	11.136
			2,000	20	5.5	14,115			
16(7+6+4)	80	82.5	2,000	20	5.5	14,115	326.21	3.74	9.778
			2,247	20	2.5	12,347			
			1,000	20	2.5	6,759			
17(7+6+4)	85	82.5	2,000	20	5.5	14,115	326.21	2.73	9.778
			2,247	20	2.5	12,347			
			1,000	20	2.5	6,759			
18(7+6+4)	90	88.5	2,000	20	5.5	14,115	401.58	1.48	12.596
			2,247	20	2.5	12,347			
			2,247	20	2.5	12,347			

whereas their actual numbers and characteristics were determined from the typically observed rainfall rate and the vertical distribution of temperature and moisture of a tropical disturbance. The numerical cloud model served as the linking agent that combined all of these observations into a coherent model of the cloud population that is determined by the large-scale flow.

The second type of interaction (that by which the clouds modulate and alter the synoptic scale) now will be explored further by computing a heat and moisture budget for a typical tropical disturbance.

One of the most interesting features of tropical disturbances is the fact that, despite the copious amounts of rain produced in a day, the majority of the storms travel for hundreds of miles over the oceans without apparent change in intensity. Williams and Gray (1973) have considered a sample of 1,257 individual satellite-observed trade-wind clusters over the Pacific Ocean. Of these, 537 were classified as conservative, 166 developed into tropical storms or typhoons, and the rest were either in the formative or dying stages. While the conservative clusters were tracked in the satellite pictures for 12–18° of longitude, no appreciable tropospheric warming or surface-pressure falls were detected even though the rainfall was computed as 2.5 cm/day. Thus the typical tropical disturbance can be considered as constituting a quasi-steady state system. In the following, only the conservative steady-state cloud clusters will be considered.

Interaction of a Steady-State Cloud Cluster as a Whole With the Environment

Since the steady-state condition implies that the total moisture content of the entire system must stay constant, the same amount of water that precipitates out of the clouds of such a disturbance must be brought in from the outside in the form of evaporation from the ocean surface and by low- and middle-level synoptic water-vapor convergence. Conversely, the heat released by the condensation of this rainwater must be exported to the exterior of the cluster if the steady-state balance is to be met. The mechanism by which this is accomplished, however, is not direct. First, the latent heat of condensation is converted into potential energy insomuch as air from lower levels is lifted up and carried aloft inside the clouds. Because of this vertical mass transport, a convergence zone is produced at the top of the disturbance that generates an outflow region at high levels. Finally, potential energy is exported to the outside as mass leaves the disturbance. Under steady-state conditions, the potential energy advected from the disturbance plus the long-wave radiational losses must be equal to the energy released through the condensation of rainwater.

The mass that leaves the disturbance at its outflow layer must be compensated by a region of convergent inflow farther down. Actually, Williams and Gray (1973) have found mass convergence into the conservative clusters all the way from the surface to 400 mb. Furthermore, this low- and middle-level convergence brings into the disturbance the water vapor necessary to establish the observed net rainfall rates. Accordingly, the water-vapor convergence into the conservative clusters was found by Williams and Gray to be equivalent to a rainfall rate of 2 cm/day. Forty-three percent of this moisture convergence occurred below 900 mb while 57 percent was found to come from convergence in the layer between 900 and 400 mb.

In general, we can view the steady-state tropical cluster (on the whole) as a system that takes in the latent heat contained in the low and middle level water-vapor convergence, converts this latent heat into potential energy, and (after subtracting the net long-wave radiational losses) exports potential energy to the environment at the layer of divergent mass outflow. With these heat-, water-, and mass-balance restrictions imposed on the cluster as a whole, the different effects (detrainment and subsidence) of the individual clouds on the cluster's atmosphere should cancel one another so that no change in the mean vertical profiles of temperature and moisture should be apparent.

Divergence Pattern Induced by the Model Cloud Population

Figure 7 portrays the vertical profile of divergence imposed on the environment surrounding the cumulus cloud population of figure 5. This profile was computed from eq (20). A low-level convergence into the clouds of

529-411 O - 74 - 4

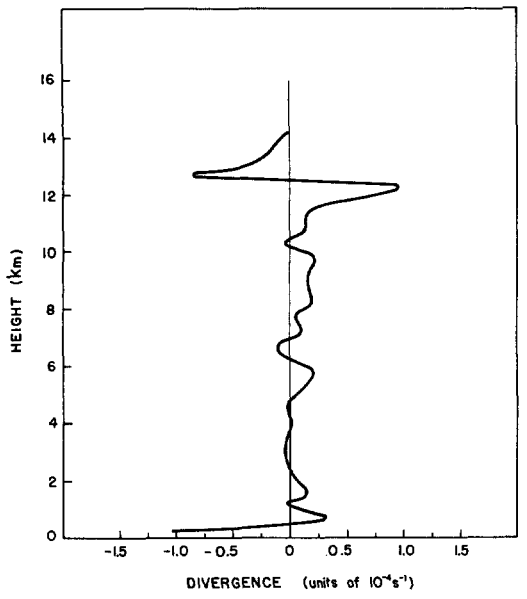

FIGURE 7.—Vertical profile of divergence imposed on a tropical cloud cluster by the upward mass transport performed by the cloud population of figure 5, assuming a low-level convergence of $10^{-4}s^{-1}$.

$10^{-4}s^{-1}$ has been assumed. As noted before, this high convergence is necessary to explain a production of about 2.5 cm of rain per day over the disturbance region. The convergence and divergence produced in the region surrounding the clouds is concentrated at very low and very high altitudes while, in the intervening regions, the effect is much smaller. The convergence at very low levels is the reflection of the mass-sink that results from the continuous ascent of low-level air into the base of the growing clouds. As these growing clouds penetrate through the environment, the surrounding air is pushed aside and local mass sources are produced along the path of the ascending currents. However, as the source of low-level air is gradually cut off for some clouds and while the tops of the clouds are still bouyant, local mass sinks are induced in the environment as a result of the shrinking radius of the stretched cloud stems. These two effects tend to cancel among clouds of different growth stages and sizes so that, in the mean, no marked convergence or divergence is observed throughout most of the cloud layer. The cloud air penetrating high altitudes, however, accumulates continually at the equilibrium level of the high clouds. Consequently, a region of high horizontal *divergence* is induced in the environment at about 12 km. The large clouds show an anvil at this location. The large *convergence* at about 13–14 km results from the fast subsidence of negatively buoyant cloud air that has overshot the equilibrium position and captured surrounding air particles. A large amount of entrained environmental air is brought down from higher levels together with the descending cloud mass. This sinking motion tends to further emphasize the large divergence of mass at about 12 km. This large divergence region has also been observed by Williams and Gray (1973), Reed and Recker (1971), and Yanai et al. (1973). To explore the implications of this effect on the vertical transport of horizontal momentum as well as on the dynamics of severe storms under vertical wind shear would be interesting.

The divergence field that results from the growth of the clouds will induce a downward flow of mass *around the clouds* to compensate for their upward mass transport. In this descending branch of the convective circulation, potential energy is converted into sensible heat, and the temperature of the environment is raised. The resultant warming, however, will be compensated by the cooling produced from the evaporation of detrained cloud water and by the cooling resulting from long-wave radiational loses.

The divergence profile presented in this section is not to be compared with the synoptic profiles that have been obtained for tropical disturbances by Williams and Gray (1973) and by Reed and Recker (1971). The present profile is a result of the upward mass transport of the clouds alone and does not include the effect of the downward sinking motion that will be induced in the clear areas around the clouds. The difference between the upward and downward mass transports produces the large-scale divergence profiles reflected in the synoptic data. The problem of the compensatory sinking motions in the clear areas around the clouds and the net divergence profile produced will be considered in this section.

Interaction of the Model Cloud Population With the Disturbance's Atmosphere

In computing a heat and water budget for the interior of the disturbance, the principal feature to be considered is the compensatory descending current that will be induced in the cloud-free region around the convective element as a result of the divergence-convergence pattern established by the clouds. The resulting dry adiabatic compression will release sensible heat to the environment ($dT_{\text{subsidence}}$). This heating will be compensated by cooling due to evaporation of cloud liquid-water ($dT_{\text{detrainment}}$) and by long-wave radiational loses ($dT_{\text{radiation}}$). The sinking motion will also result in the drying of the cloud-free regions ($dX_{\text{subsidence}}$). This will similarly be compensated by the detrainment of water vapor and liquid water from the different types of clouds present ($dX_{\text{detrainment}}$). The advection of environmental mass into the disturbance's atmosphere is another source of heat ($dT_{\text{advection}}$) and moisture ($dX_{\text{advection}}$) that should be included in the heat and water budgets.

We can express the change in temperature of a horizontal slab of the cloud cluster's atmosphere in a quantitative form as

$$dT=dT_{\text{subsidence}}+dT_{\text{radiation}}+dT_{\text{advection}}+dT_{\text{detrainment}}. \quad (21)$$

The change in temperature due to subsidence can in turn

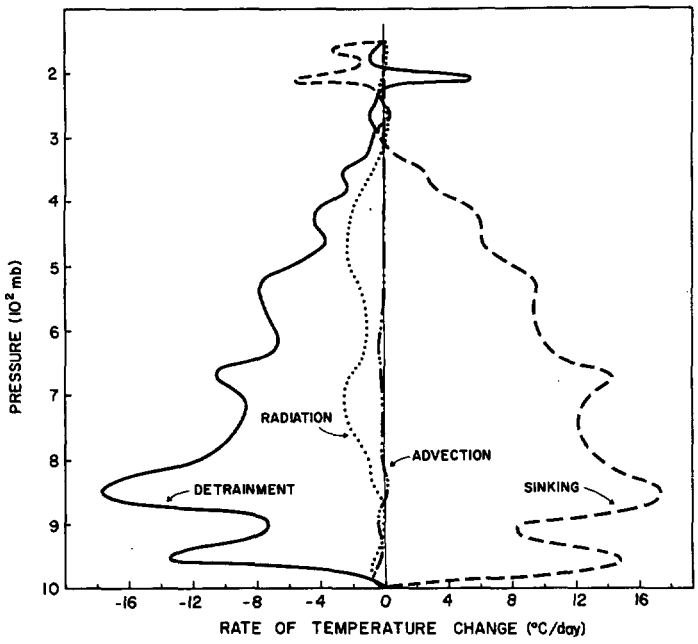

FIGURE 8.—Vertical profiles of the different heating terms of the heat budget of a steady-state tropical cloud cluster.

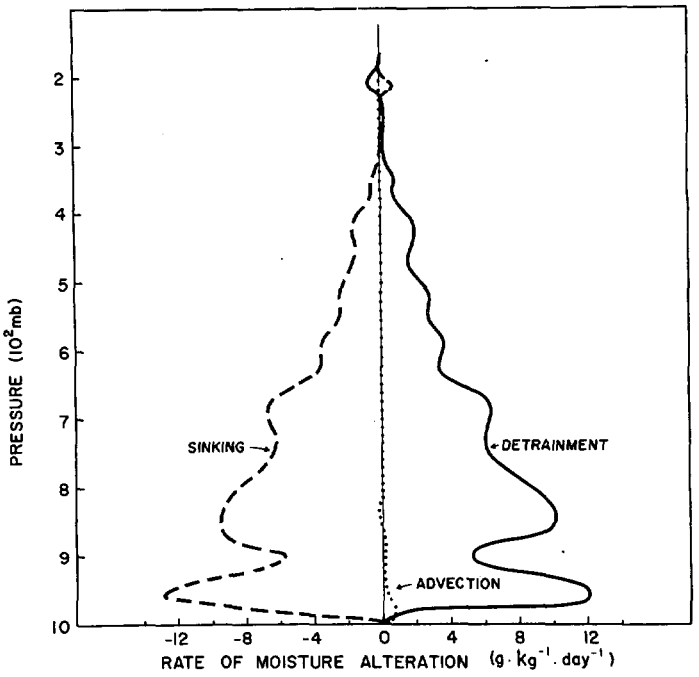

FIGURE 9.—Same as figure 8 except this is for the moisture budget.

be written as

$$dT_{\text{subsidence}}=\left(\frac{dT}{dz}-\frac{g}{c_p}\right)W_s dt \qquad (22)$$

where dT/dz is the lapse rate of the cluster; g/c_p, the dry adiabatic lapse rate; W_s, the vertical velocity of the cloud-free regions within the disturbance; and dt, a small interval of time. The vertical velocity W_s can be obtained from the vertical integration of the divergence profile presented in figure 7 after provision is made for the advection of mass in and out of the disturbance by the synoptic divergence profile. The radiation term has been obtained from tropical data presented by Cox (1969). His infrared cooling profile for low-, middle-, and high-cloud conditions was believed adequate for the representation of the long-wave radiation processes in a tropical cloud cluster. The corresponding short-wave warming profile was computed for similar cloudiness structures using the radiation model described in Manabe and Strickler (1964).

The change in temperature due to advection of environmental air into the disturbance can be expressed as

$$dT_{\text{advection}}=(T_{\text{environment}}-T_{\text{disturbance}})\frac{dm_{ad}}{m} \qquad (23)$$

where dm_{ad} is the amount of mass advected into the disturbance during a small interval of time dt and m is the mass of a layer of the cluster. This advected mass can be evaluated from the convergence profile obtained by Williams and Gray (1973) for conservative cloud clusters. The changes in temperature due to detrainment from the clouds can be obtained from eq (13).

The change in the mixing ratio of water vapor of a horizontal layer or slab of the disturbance can also be expressed in the form

$$dX=dX_{\text{subsidence}}+dX_{\text{advection}}+dX_{\text{detrainment}}. \qquad (24)$$

The contribution due to subsidence is

$$dX_{\text{subsidence}}=\frac{dX}{dz}W_s dt \qquad (25)$$

where dX/dz is the vertical gradient of mixing ratio in the cloud cluster's atmosphere and the other terms have the same meaning as in eq (22). The change in mixing ratio due to advection becomes

$$dX_{\text{advection}}=(X_{\text{environment}}-X_{\text{disturbance}})\frac{dm_{ad}}{m}. \qquad (26)$$

Similarly, the water-vapor contribution of the detrainment from the clouds can be obtained from eq (14).

Results of the Heat and Moisture Budget

Equations (21) and (24) have been integrated for a period of 24 hr in time steps of 15 min. Every 15 min, the change in temperature and moisture of 500-m-thick layers of the disturbance were found, and new temperature and mixing ratio profiles were computed. These new values were used to evaluate the new changes, and so on. Figures 8 and 9 portray the accumulated effect of each of the terms of eq (21) and (24) for the time interval of 1 day. The final temperature profile was within 0.2°C of the initial (environmental) temperature while the mixing ratio profile was within 0.1 g/kg of the initial values.

The values with height of the different terms of the *heat budget* of the disturbance are shown in figure 8. A mean tropospheric cooling of 1.0°C is experienced during a day due to radiational losses (dotted line). This cooling is

compensated by the much larger warming produced by the induced sinking motion (dashed line). This sinking produces a mean warming of 7.5°C/day, the largest warming being experienced in the lower half of the disturbance's atmosphere (18°C). Notice that, as a result of the induced ascent at high levels, a local cooling of about 5°C results at about 200 mb. The net effect of detrainment on the disturbance is a mean cooling of 6.1°C. Note how the subsidence warming is modulated by the cooling due to detrainment. This close adjustment is a result of the dependence of the subsidence-warming term on the difference between the dry adiabatic lapse rate and actual lapse rate of the disturbance [eq (22)]. As the detrainment cooling changes the lapse rate of the disturbance, the sinking warming changes in the opposite sense. As a result, there is a tendency in the long run for a close compensation of both effects. The effect of advection of environmental air is small compared to any of the other terms (approx. −0.1°C).

Considering the different terms of the humidity budget (fig. 9), one can see that there is a good balance between the subsidence and detrainment effects while the advection of environmental air contributes very little to the total moisture budget. The dryness produced by the subsidence of cloud-free air is balanced closely by the detrainment of water vapor and cloud liquid water at all levels. This close adjustment is a result of the dependence of the detrainment term on the difference between the mixing ratio of the cloud and that of the disturbance. As a result, there is a tendency for the clouds in the long run to compensate exactly for the dryness produced by subsidence.

These results show that to explain the role of cumulus clouds in the energetics of a tropical disturbance, we must consider both the ascending and descending branches of the cumulus convection circulation. The effect of the *ascending branch* (upward mass transport inside the clouds) is to cool the disturbance and increase the moisture of the disturbance by the process of detrainment and to induce a compensatory sinking motion around the clouds. The effect of the induced *descending branch* of the convective circulation around the clouds is to warm the disturbance by converting potential energy into sensible heat and to decrease the humidity of the air around the clouds by bringing down upper air of lower water vapor content.

In the quasi-steady state disturbance, the effects of the two branches of the convective circulation and of radiation balance one another so that the temperature and moisture profiles remain nearly constant in time. From the point of view of the total disturbance, the heat liberated in the condensation of the 2 or 3 cm of rain per day is used to compensate for the radiational losses, and the rest is exported as potential energy to the general tropical circulation.

Other Evidences of the Direct Cooling Action of Cumulus Clouds

Direct sensible temperature decreases, around and after cumulus convection has taken place, have been reported by Kininmonth (1970) from data of the VEMHEX project of 1969. Further evidence of the direct cooling action of cumulus clouds is the lower troposphere low temperatures found in tropical disturbances and waves of the easterlies (Riehl 1945). In part I, Gray (1973) has discussed other evidences of direct cumulus cooling. In the study of 1,000 Pacific trade-wind cloud clusters, Williams and Gray (1973) found no appreciable tropospheric warming or surface-pressure falls even through the rainfall was very large. Their average cloud cluster precipitation was computed to be 2.5 cm/day for a 4° latitude square area. The 1500 $cal \cdot cm^{-2} \cdot day^{-1}$ liberated through the condensation of this rainfall resulted in no tropospheric warming even though the ventilation of the storms was small. Recent computations by Gray (1973) also indicate that it is impossible to explain the tropospheric sensible temperature balance around the globe without invoking a direct cloud sensible cooling that averages about two-thirds of the net tropospheric radiational cooling.

Cooling Tower Hypothesis

The results of the computations performed in this section indicate that, by itself, detrainment from active cumuli produces a net cooling of the air in which the clouds are embedded. The evaporation of detrained liquid water overcompensates for any direct detrainment of sensible heat from the clouds. Even in the case of vigorous cumulonimbi with temperature excesses of 5° and 6°C, enough liquid water is present to produce a net cooling effect on the environment. If the results of the computations presented here are verified, the classical view of cumulus clouds providing heat to the environment through direct diffusion (Riehl and Malkus 1958) must be revised. It appears that, as a result of detrainment alone (direct diffusion of cloud mass), cumulus clouds act as cooling towers instead of performing the often hypothesized warming role (Ooyama 1963, Charney and Eliassen 1964, Ogura 1964, Kuo 1965, Rosenthal 1970). This point of view has also been expressed by Gray (1973).

Vertical Mass Circulation in a Steady-State Disturbance

Figure 10 portrays the different components of the vertical mass circulation present in a steady-state disturbance. Curve A (solid line) represents the mean upward mass transport that the model cloud population must perform to produce a rainfall rate of 2.5 cm/day. This means that the mass transport by the clouds establishes the divergence profile shown in figure 7. Curve B (dash-dot line) represents the upward mass transport resulting from the synoptic divergence profile of Williams and Gray (1973). The difference between the *required* (curve A) and the *synoptic* (curve B) upward mass transport must be compensated locally *inside* the disturbance by a downward mass transport in the clear regions between clouds. This downward mass circulation is portrayed in curve C (dotted line). This sinking motion releases

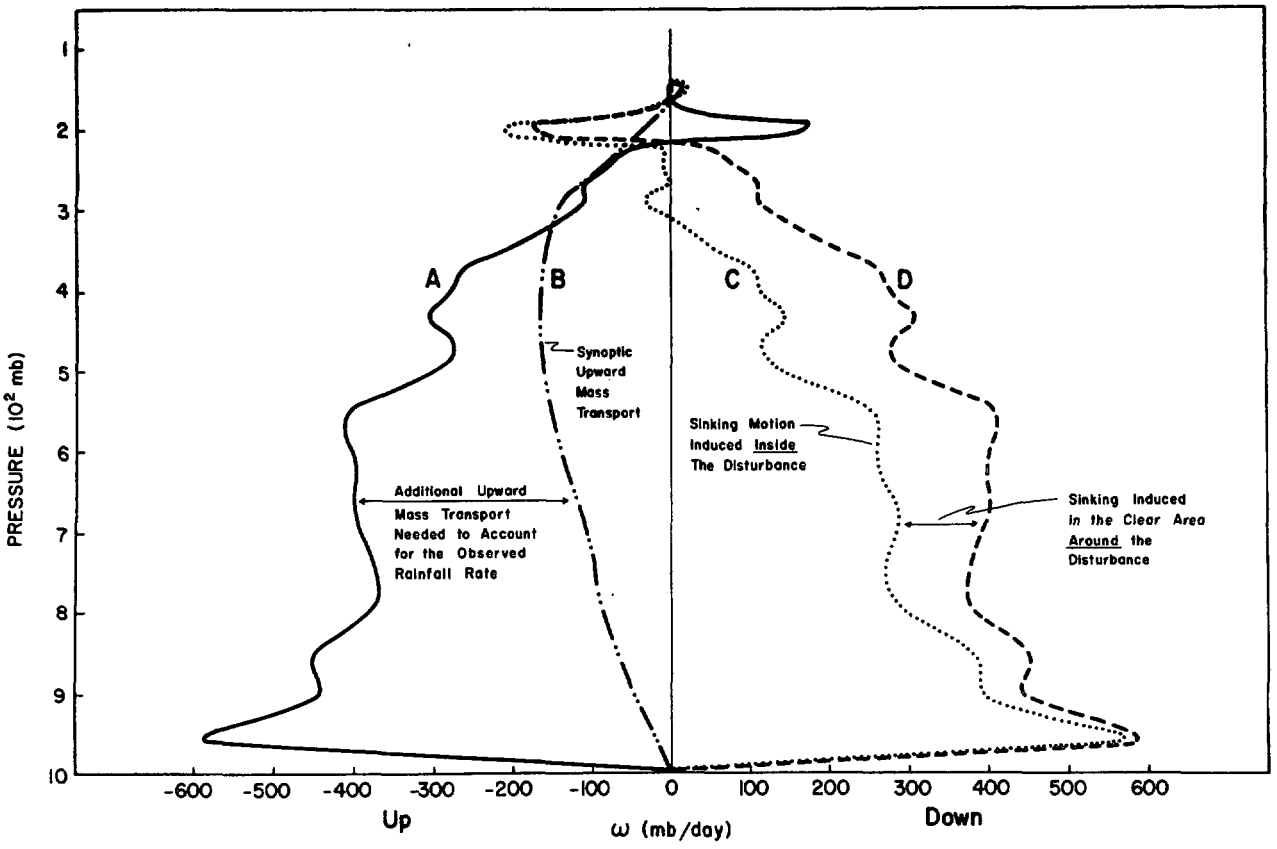

FIGURE 10.—Different components of the vertical mass circulation present in a steady-state cloud cluster.

sensible heat to the disturbance's atmosphere, as noted previously. The compensation for the remaining upward mass circulation (the synoptic contribution) occurs *outside* the disturbance. Adding this downward-outside contribution to curve C, we obtain the total downward branch of the mass circulation of the disturbance (curve D). For illustration, we assumed that the subsidence occurring outside takes place over an area equal to that of the disturbance.

Role of Recycling in Generation of Individual Cumulus Elements

The general stability of the cloud cluster lower layers and the need for a lifting mechanism to initiate parcel condensation until free convection is obtained are generally accepted. Over the ocean, these conditions require the application of substantial mechanical forcing to initiate buoyant elements. As discussed by López (1973), to generate cumulus over the oceans without cloud base vertical velocities of 1–5 m/s is impossible. This is equivalent to having local convergences during the cloud's growing stages of about $3\text{–}6\times10^{-3}s^{-1}$. These values are 1,000–2,000 times larger than the synoptic convergence. Even if the active cumulus take up only 1 percent of the cluster area, these convergences are 10–20 times larger than that specified by synoptic convergence. The only way the extra convergence under the cluster cumulus can occur is by a large mass recycling mechanism, which is 10–20 times greater than the synoptic mass convergence.

The recycling dry and moist downdraft air that penetrates into the boundary layer from upper levels is believed to be the primary mass source for cloud parcel initiation. Were the cluster cumulus to be initiated or forced only by the synoptic convergence of $3\text{–}5\times10^{-6}s^{-1}$, then low-level mass requirements would permit only about 1/1,000 of the cluster area to be occupied by parcel ascent if all the mass sent into cumulonimbi (or only about 1/500 of the area) is occupied by all towering cumulus or by all cumulus parcel ascent. The radar data presented in this paper show that the areas of the cluster occupied by active cumulus clouds are typically 10–20 times larger than these amounts. The fundamental requirement of large up-and-down mass recycling 10–20 times larger than the mean vertical mass flow at cloud base is clearly evident, given the typical cloud cluster synoptic convergences and stable lapse rate conditions.

Developing Cloud Clusters

The preceding computations apply to the case of a steady-state tropical disturbance [i.e., a system that exports at high altitudes (in the form of potential energy) the latent heat advected into it at low and middle levels]. This type of dsturbance represents the typical cloud cluster that travels for several days over the oceans with no appreciable change in intensity. The heat liberated in the condensation of the 2 or 3 cm of rain produced in a day is exported as potential energy to the general tropical circulation in which the cloud cluster is embedded, after provision is made for the disturbance's own radiational losses.

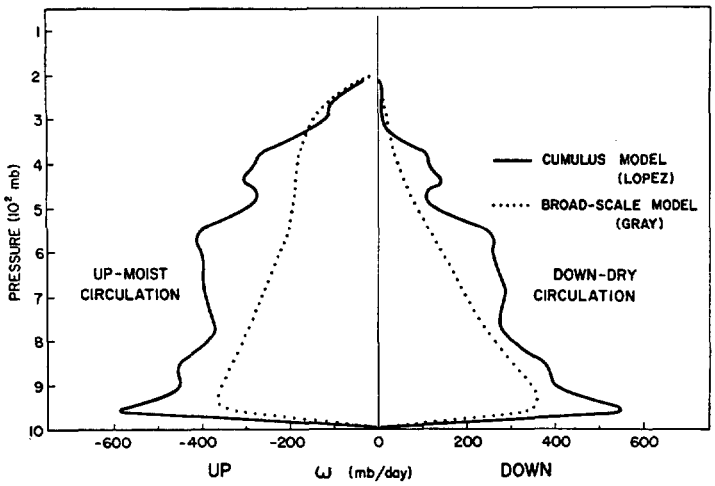

FIGURE 11.—Comparison of the cloud cluster vertical circulation as determined in this paper and with similar values obtained by Gray (1973).

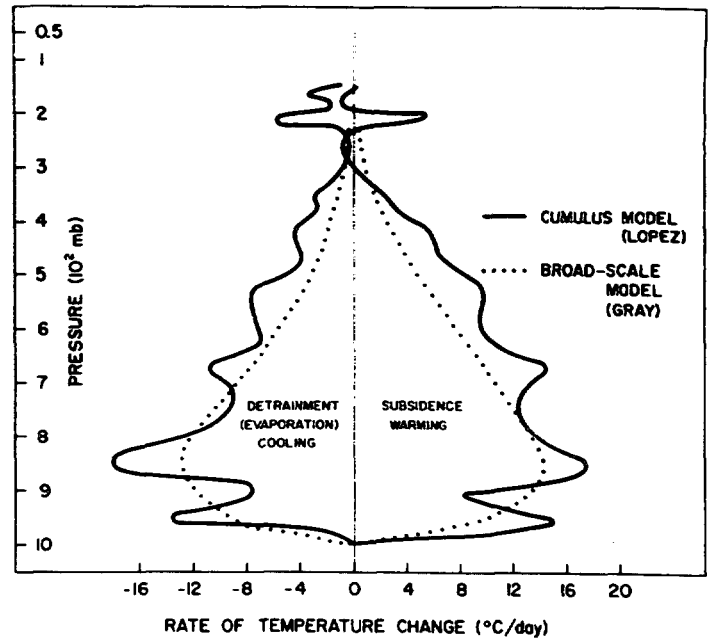

FIGURE 12.—Comparison of each model's subsidence warming and evaporation cooling.

The response of the large-scale flow to the energy exportation of a disturbance, however, can result in drastic changes in the synoptic features of the region. This is the case of hurricane development. The interaction between a disturbance and the surrounding flow can be viewed in the following way: A tropical disturbance as a whole takes in environmental mass at low and middle levels and exports mass at high altitudes. A compensatory sinking motion is induced in the air surrounding the disturbance to satisfy the synoptic upward mass transport of the disturbance as a whole. In this way, the potential energy produced by the cloud cluster as a whole is converted into sensible energy outside the cluster. The degree of the resultant warming depends, however, on the scale on which the compensatory sinking occurs. If the subsidence takes place over a broad region, a slight warming is experienced, which is probably used to compensate for the radiational cooling of the area. If the compensatory subsidence occurs over a small region near the disturbance, however, enough compressional warming could take place to explain hurricane development. In fact, Oliver and Anderson (1969) have found from satellite observations that the majority of hurricanes form around a circulation center that develops in the *clear area* ahead of the convective region. The study of the large-scale flow features leading to a concentrated compensatory descending current is beyond the scope of this investigation. There are reasons to believe, however, that the broadscale flow at the level of the disturbance's outflow (approx. 200 mb) might be the controlling factor. Thus if the wind pattern at that level allows the outflow from the disturbance to be spread over a broad region, only gentle subsidence and warming will occur. However, if the upper air wind pattern restricts the outflow, strong local subsidence and considerable warming might develop near the disturbance. The convective activity would then organize itself around the resulting warm core low-pressure region. Further studies along these lines could provide considerable insight into the physics of hurricane development from weak tropical disturbances.

6. COMPARISON OF THE BUDGETS COMPUTED IN THIS PAPER WITH SIMILAR BUDGETS COMPUTED FROM SYNOPTIC DATA ALONE

In part I, Gray (1973) has discussed the heat and moisture budgets and vertical circulation of the mean tropical cloud cluster of the Pacific. His computations were based entirely on composited synoptic data without any cumulus scale information. His results will now be compared with the budgets and vertical circulation obtained in this paper, which were based on detailed knowledge of individual cumulus clouds of different types and empirically derived cumulus populations.

Figures 11, 12, and 13 show the comparison of the two methods with regard to their local vertical circulations, heat budgets, and moisture budgets, respectively. One can clearly see how well these models agreed in specifying the required mass, energy, and water-vapor budgets. This lends consistency and credibility to the results of each approach. This inward meshing of the dynamics from opposite scales of consideration should always be a desirable goal for ultimately verifying cumulus broader scale interaction models.

These two computations were done independently. The two methods used are very different from each other since they reflect two completely different approaches to the study of cumulus larger scale interactions. The fact that the end results of the computations agree so well,

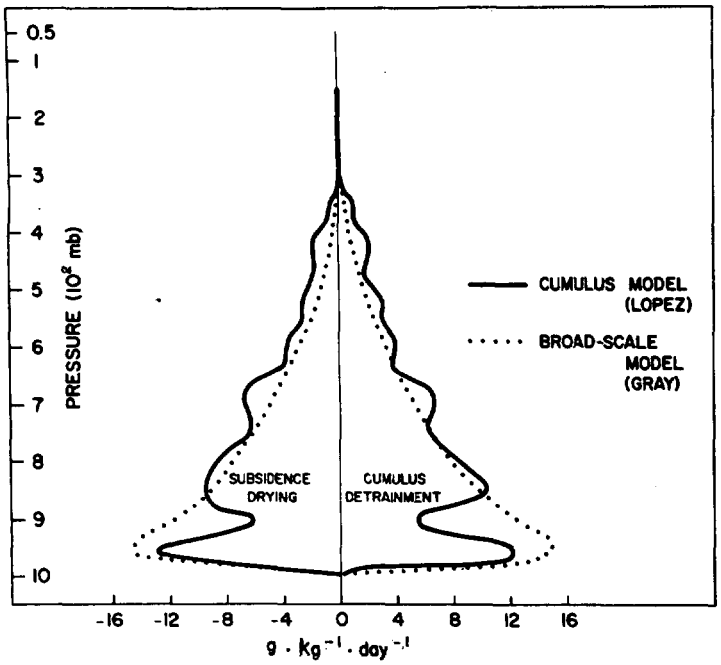

FIGURE 13.—Comparison of each model's water-vapor budget.

despite the varying methodologies, is strong evidence for the correctness of both treatments.

7. SUMMARY

A numerical model of individual cumulus clouds has been used in this section to investigate the effects of cumulus convection on the large-scale features of tropical disturbances or cloud clusters. A cloud population characteristic of tropical cloud clusters has been determined from radar and synoptic observations. With the help of the numerical cloud model, the effects of the typical ensemble of cumuli have been calculated. One major effect consists of the detrainment of cloud mass, which will cause a direct transport of excess sensible heat as well as cooling of the surrounding clear air as a result of the evaporation of the detrained cloud liquid water. The net effect was found to be one of cooling as the evaporation overcompensates for the detrainment of excess sensible heat. In this regard, cumulus clouds should be considered as a basic cooling tower as opposed to a hot tower concept. The other effect produced by the typical population is the induction of a descending motion in the environment to compensate for the upward mass transport of the clouds. The induced subsidence will result in the warming and drying of the environment.

Using all of this information, we computed a heat and moisture budget for a steady-state tropical disturbance. Under steady-state assumptions, the heat liberated from the condensation of rainwater is exported to the environment in the form of potential energy at the level of the disturbance's outflow. At the same time, the water vapor necessary to produce the rainfall is imported into the disturbance in the form of a low- and middle-level mass convergence. Inside the disturbance, the warming resulting from the sinking motion is compensated by the net cooling resulting from detrainment plus the cooling resulting from infrared radiational losses. Similarly, the dryness resulting from the subsidence is compensated by the detrainment of water vapor and liquid water from the clouds.

The convergence of mass at low and middle levels *into* the disturbance as a whole and the high-altitude outflow of mass *from* the disturbance will, in turn, induce a descending motion in the clear air surrounding the storm. The warming will be large or small depending on the scale at which the subsidence occurs. Under favorable situations, the warming could be large enough to produce hydrostatically the low pressures needed for the organization of a tropical disturbance into a full-fledged hurricane. The present numerical model of cumulus clouds has proven to be useful in investigating the interaction of cumuli with the large-scale features of tropical disturbances, and future investigations using this tool are expected to result in the clarification of the problem of formation of hurricanes from a weaker disturbance and in the maintenance of the tropical general circulation.

ACKNOWLEDGMENTS

The author wishes to express his sincere gratitude to William M. Gray under whose guidance this investigation was performed. His kind criticism and encouragement are very much appreciated. Special thanks are due to Edward Buzzel, Barbara Brumit, and Larry Kovacic who helped with the programming, manuscript typing, and drafting.

REFERENCES

Battan, Louis J., "Duration of Convective Radar Clouds," *Bulletin of the American Meteorological Society*, Vol. 34, No. 5, May **1953**, pp. 227–228.

Blackmer, Roy H., Jr., "The Lifetime of the Small Precipitation Echoes Observed on the PPI Scope of the SCR–615–B Radar," *Proceedings of the 5th Weather Radar Conference, Asbury Park, N.J.*, American Meteorological Society, Boston, Mass., **1956**, pp. 103–108.

Charney, Jule G., and Eliassen, Arnt, "On the Growth of the Hurricane Depression," *Journal of the Atmospheric Sciences*, Vol. 21, No. 1, Jan. **1964**, pp. 68–75.

Cox, S. K., "Radiation in the Free Atmosphere," Contract No. E 22–113–68(G), Department of Meteorology, The University of Wisconsin, Madison, **1969**, 68 pp.

Gray, William M., "Cumulus Convection and Larger Scale Circulations I. Broadscale and Mesoscale Considerations," *Monthly Weather Review*, Vol. 101, No. 12, Dec. **1973**, pp. 839–855.

Holle, Ronald L., "Some Aspects of Tropical Oceanic Cloud Populations," *Journal of Applied Meteorology*, Vol. 7, No. 2, Apr. **1968**, pp. 173–183.

Kininmonth, W. R., "Thermal Modification of the Troposphere Due to Convective Interaction," *Atmospheric Science Paper* No. 167, Department of Atmospheric Science, Colorado State University, Fort Collins, **1970**, 36 pp.

Kuo, H. L., "On Formation and Intensification of Tropical Cyclones Through Latent Heat Release by Cumulus Convection," *Journal of the Atmospheric Sciences*, Vol. 22, No. 1, Jan. **1965**, pp. 42–63.

López, Raúl E., "Investigation of the Importance of Cumulus Convection and Ventilation in Early Tropical Storm Development," *Atmospheric Science Paper* No. 124, Department of Atmospheric Science, Colorado State University, Fort Collins, June **1968**, 86 pp.

López, Raúl E., "A Parametric Model of Cumulus Convection," *Atmospheric Science Paper* No. 188, Department of Atmospheric Science, Colorado State University, Fort Collins, **1972**, 190 pp.

López, Raúl E., "A Parametric Model of Cumulus Convection," (Paper A), *Journal of the Atmospheric Sciences*, Vol. 30, No. 7, Oct. **1973**, pp. 1354–1373.

Manabe, Syukuro, and Strickler, Robert G., "Thermal Equilibrium of the Atmosphere With a Convective Adjustment," *Journal of the Atmospheric Sciences*, Vol. 21, No. 4, July **1964**, pp. 361–385.

McIntyre, H. D., "Radar Study of the Motion of Small Precipitation Areas in Hurricanes 'Carol' and 'Edna'," *Technical Note* No. 9, Department of Meteorology, Massachusetts Institute of Technology, Cambridge, **1956**, pp. 4–5.

Ogura, Yoshimitsu, "Frictionally Controlled, Thermally Driven Circulations in a Circular Vortex With Application to Tropical Cyclones," *Journal of the Atmospheric Sciences*, Vol. 21, No. 6, Nov. **1964**, pp. 610–621.

Oliver, Vincent J., and Anderson, Ralph K., "Circulation in the Tropics as Revealed by Satellite Data," *Bulletin of the American Meteorological Society*, Vol. 50, No. 9, Sept. **1969**, pp. 702–707.

Ooyama, Katsuyuki, "A Dynamical Model for the Study of Tropical Cyclone Development," Contract No. 65–12, Department of Meteorology and Oceanography, New York University, Bronx, **1963**, 26 pp.

Ooyama, Katsuyuki, "Numerical Simulation of the Life Cycle of Tropical Cyclones," *Journal of the Atmospheric Sciences*, Vol. 26, No. 1, Jan. **1969**, pp. 3–40.

Reed, Richard J., and Recker, Ernest E., "Structure and Properties of Synoptic-Scale Wave Disturbances in the Equatorial Western Pacific," *Journal of the Atmospheric Sciences*, Vol. 28, No. 7, Oct. **1971**, pp. 1117–1133.

Riehl, Herbert, "Waves in the Easterlies and the Polar Front in the Tropics," *Miscellaneous Reports* No. 17, Department of Meteorology, University of Chicago, Ill., **1945**, 79 pp.

Riehl, Herbert, and Malkus, Joanne S., "On the Heat Balance in the Equatorial Trough Zone," *Geophysica*, Vol. 6, No. 314, Helsinki, Finland, **1958**, pp. 503–538.

Rosenthal, Stanley L., "A Circularly Symmetric Primitive Equation Model of Tropical Cyclone Development Containing an Explicit Water Vapor Cycle," *Monthly Weather Review*, Vol. 98, No. 9, Sept. **1970**, pp. 643–663.

Senn, H. V., Hiser, H. W., and Low, E. F., "Studies of the Evolution and Motion of Hurricane Spiral Bands and the Radar Echoes Which Form From Them," The Marine Laboratory, University of Miami, Coral Gables, Fla., Aug. **1959**, 65 pp.

Senn, H. V., and Stevens, J. A., "A Summary of Empirical Studies of the Horizontal Motion of Small Radar Precipitation Echoes in Hurricane Donna and Other Tropical Storms," *Report* No. 74, National Hurricane Research Laboratory, National Oceanic and Atmospheric Administration, U.S. Department of Commerce, Coral Gables, Fla., **1965**, 55 pp.

Williams, K. T., and Gray, William M., "A Statistical Analysis of Satellite-Observed Trade Wind Cloud Clusters in the Western North Pacific," *Tellus*, Vol. 25, No. 4, Stockholm, Sweden, **1973** (in press).

Yanai, Michio, Esbensen, Steven, and Chu, Jan-Hwa, "Determination of Bulk Properties of Tropical Cloud Clusters From Large-Scale Heat and Moisture Budgets," *Journal of the Atmospheric Sciences*, Vol. 30, No. 4, May **1973**, pp. 611–627.

[Received September 22, 1972; revised September 29, 1973]